Ultrasonics Sonochemistry 24 (2015) 221–229

Contents lists available at ScienceDirect

Ultrasonics Sonochemistry

journal homepage: www.elsevier.com/locate/ultson

Sonophotocatalytic degradation of dye C.I. Acid Orange 7 by TiO_2 and Ag nanoparticles immobilized on corona pretreated polypropylene non-woven fabric

Darka Marković [a], Zoran Šaponjić [b], Marija Radoičić [b], Tamara Radetić [c], Vesna Vodnik [b], Branislav Potkonjak [d], Maja Radetić [c,*]

[a] Innovation Center, Faculty of Technology and Metallurgy, University of Belgrade, Karnegijeva 4, 11000 Belgrade, Serbia
[b] Vinča Institute of Nuclear Sciences, University of Belgrade, P.O. Box 522, 11001 Belgrade, Serbia
[c] Faculty of Technology and Metallurgy, University of Belgrade, Karnegijeva 4, 11000 Belgrade, Serbia
[d] Institute of Chemistry, Technology and Metallurgy, University of Belgrade, Njegoševa 12, 11000 Belgrade, Serbia

ARTICLE INFO

Article history:
Received 26 August 2014
Received in revised form 6 November 2014
Accepted 19 November 2014
Available online 27 November 2014

Keywords:
Polypropylene
Non-woven fabric
Corona discharge
TiO_2 nanoparticles
Ag nanoparticles
Sonophotocatalysis

ABSTRACT

This study discusses the possibility of using corona pre-treated polypropylene (PP) non-woven fabric as a support for immobilization of colloidal TiO_2 and Ag nanoparticles in order to remove dye C.I. Acid Orange 7 from aqueous solution. Dye removal efficiency by sonocatalysis, photocatalysis and sonophotocatalysis was evaluated on corona pre-treated fabric loaded with TiO_2 nanoparticles, corona pre-treated fabric double loaded with TiO_2 nanoparticles and corona pre-treated fabrics loaded with TiO_2 nanoparticles before and after deposition of Ag nanoparticles. In addition, the stability of PP non-woven fabric during these processes was investigated. The substrates were characterized by SEM, EDX and AAS analyses. The change of the dye concentration was evaluated by UV–VIS spectrophotometry. Unlike sonocatalysis and photocatalysis, complete dye removal from both solution and non-woven fabric was obtained already after 240–270 min of sonophotocatalysis. Corona pre-treated PP non-woven fabric loaded with Ag nanoparticles prior to deposition of TiO_2 nanoparticles provided excellent degradation efficiency and superior reusability. Sonophotocatalytic degradation of dye in the presence of all investigated samples was the most prominent in acidic conditions. Although this nanocomposite system ensured fast discoloration of dye solution, TOC values of water measured after sonophotocatalysis were not satisfactory because of PP degradation. Therefore, it is suggested to include TOC evaluation in each case study where different supports for TiO_2 nanoparticles are used since these nanoparticles may guarantee the dye removal from solution but the stability of support could be problematic causing even more serious environmental impact.

1. Introduction

Negative environmental impact of municipal and particularly industrial effluents became the issue of serious global concern. Elimination of the effluent pollution requires efficient and cost effective solutions. Industrial effluents commonly contain various toxic organic compounds that are highly stable and mostly resistant to conventional wastewater treatments [1]. Advanced Oxidation Processes (AOPs) such as heterogeneous photocatalysis, Fenton and photo-Fenton oxidation, ozonation, sonolysis and UV/H_2O_2 treatment are very efficient methods for oxidation and mineralization of many resistant organic contaminants [2–6]. AOPs rely on generation and action of highly reactive hydroxyl radicals ($OH^{\cdot}$) which possess great oxidative potential. Hence, they are able efficiently to oxidize organic pollutants and mineralize them to carbon dioxide, water and mineral acids.

Recently, environmental sonochemistry gained much attention due to its safety, cleanness, high penetration ability through aquatic medium and high degradation efficiency without generation of secondary pollutants [1]. Ultrasound has been utilized for degradation of different pollutants including phenols, pesticides, herbicides, pharmaceuticals, organic dyes and pathogenic bacteria [7]. High cost is the major obstacle for industrial scale application of the ultrasound in wastewater treatment. It has been reported that overall cost of the ultrasound exploitation in phenol, dyes and

* Corresponding author at: Faculty of Technology and Metallurgy, University of Belgrade, Karnegijeva 4, 11120 Belgrade, Serbia. Tel.: +381 11 3303 857; fax: +381 11 3370 387.
E-mail address: maja@tmf.bg.ac.rs (M. Radetić).

http://dx.doi.org/10.1016/j.ultsonch.2014.11.017
1350-4177/

trichloroethylene degradation is significantly higher compared to the one that comes up when ultrasonic treatment is combined with other AOPs. Recent studies revealed that combination of sonolysis and heterogeneous photocatalysis i.e., sonophotocatalysis enhances the degradation rate of some organic compounds [1–8]. In other words, sonophotocatalysis seems to be more efficient than sonolysis or photocatalysis alone [6,8]. Both processes generate $OH^{\cdot}$ radicals but through different reaction mechanisms. Ultrasound cavitations induce splitting of water molecules into the $H^{\cdot}$ and $OH^{\cdot}$ radicals. In the case of photocatalysis, $OH^{\cdot}$ radicals are created in the reaction of positive holes generated on the photocatalyst surface under UV irradiation and water molecules [1,6,9]. Synergistic effect of these processes becomes prominent at low ultrasound frequencies (20–100 kHz) and when the photocatalysts is applied in the form of small particles [10]. Namely, particles of photocatalyst facilitate the cavitation phenomena by breaking up the microbubbles into smaller ones. On the other hand, mechanical effect of ultrasound waves induces deaggregation and cleaning of photocatalyst particles. In addition, it increases the mass transfer of pollutant between the solution phase and photocatalyst surface.

Although very efficient in wastewater treatment, photocatalyst nanoparticles are not convenient for the practical use as they require expensive liquid–solid separation due to formation of milky dispersions after mixing with water. In order to avoid additional post-treatment, the immobilization of nanoparticles on various supports is seen as a reasonable solution [11–15]. A wide range of materials have been evaluated as supports including glass [16], activated carbon [17], silica material [18] and polymeric materials [19]. Boutoumi et al. demonstrated that loading of montmorillonite with TiO_2 nanoparticles (TiO_2 NPs) ensured sonophotocatalytic degradation of dye Rhodamine 6G [11]. It was also reported that TiO_2 NPs immobilized on polypropylene (PP) fibers showed higher stability and photodegradation ability than TiO_2 NPs immobilized on Pyrex glass [14].

This study discusses the possibility of immobilization of colloidal TiO_2 NPs on the PP non-woven fabric in order to provide degradation of synthetic dye C.I. Acid Orange 7 in aqueous medium by sonocatalysis, photocatalysis and sonophotocatalysis. In addition, the stability of PP non-woven fabric as a support during these processes was investigated. The material based on PP fibers was chosen as a substrate for NPs immobilization due to good mechanical properties of PP fibers, their thermal resistance and resistance to alkalis and acids, low cost and recyclability [20–22]. PP fibers are hydrophobic in nature and quite inert. Hence, prior to impregnation with colloidal TiO_2 NPs, non-woven fabric was modified by corona discharge at atmospheric pressure. Introduction of polar groups on the surface of PP fibers would enhance the binding of hydrophilic colloidal TiO_2 NPs. In addition, PP fibers were loaded with small amount of Ag NPs since their presence can facilitate the photocatalytic activity of TiO_2 NPs.

2. Experimental

2.1. Materials

PP non-woven fabric (40 g/m^2) was used as a substrate for immobilization of colloidal TiO_2 and Ag NPs. In order to remove the surface impurities, the sample was immersed in ethyl alcohol (Zorka, Serbia) for 10 min at liquor-to-fabric ratio of 40:1 and rinsed with tap and distilled water.

Corona pre-treatment of the PP material (CPP) was performed at atmospheric pressure using a commercial device Vetaphone CP-Lab MK II. PP samples were placed on the electrode roll, rotating at the minimum speed of 4 m/min. The distance between electrodes was 2.3 mm. The power was 700 W and the number of passages was set to 30.

All the chemicals used for the synthesis of colloidal solution consisting of TiO_2 NPs were analytical grade and used as received without further purification (Aldrich, Fluka). Milli-Q deionized water was used as a solvent. The colloids of TiO_2 NPs were prepared in a manner analogous to the one proposed by Rajh et al. [23]. The solution of $TiCl_4$ cooled up to −20 °C was added dropwise to cooled water (at 4 °C) under vigorous stirring and then kept at this temperature for 30 min. The pH of the solution was in the range 0–1, depending on $TiCl_4$ concentration. Slow growth of the particles was achieved by using dialysis against water at 4 °C until the pH of the solution reached 3.5. The concentration of TiO_2 NPs colloidal solution was determined from the concentration of the peroxide complex obtained after dissolving the particles in concentrated H_2SO_4 [24]. Subsequently the colloid was thermally treated in reflux at 60 °C for 16 h.

$AgNO_3$ (Kemika) and $NaBH_4$ (Fluka) of p.a. grade were used without any further purification for the synthesis of colloid of Ag NPs. Colloidal solution consisting of Ag NPs was prepared as described elsewhere [25]. 1.7 mg of $AgNO_3$ was dissolved in 100 ml of water purged by argon for 30 min. Under vigorous stirring, reducing agent $NaBH_4$ (10 mg) was added to the solution and left for 1 h in argon atmosphere. The concentration of Ag NPs colloidal solution was 10 mg/L. In order to get concentration of 5 mg/L, freshly prepared Ag colloidal solution of 10 mg/L was mixed with deionized water (1:1). 5 mg/L Ag NPs colloidal solution was applied to CPP material.

CPP samples were impregnated with TiO_2 NPs (CPP + TiO_2) according to the following procedure: CPP sample was immersed in TiO_2 NPs colloidal solution (0.1 M) for 5 min at liquor-to-fabric ratio of 40:1, squeezed out through laboratory pad (2 kg/cm^2) and dried at room temperature. After 5 min long curing at 100 °C the samples were rinsed twice (5 min) with deionized water and dried at room temperature. This procedure was repeated one more time for getting CPP material double loaded with colloidal TiO_2 NPs (CPP + TiO_2 × 2).

CPP samples were dipped into the Ag NPs colloidal solution (5 mg/L) for 5 min at liquor-to-fabric ratio 60:1 and dried at room temperature. The liquor-to-fabric ratio in this case was higher compared to impregnation with TiO_2 NPs because the concentration of Ag NPs colloidal solution was very low. After 5 min of curing at 100 °C, the samples were rinsed twice (5 min) with deionized water and dried at room temperature. Afterwards, these samples were treated with 0.1 M TiO_2 colloidal solution (CPP + Ag + TiO_2) according to procedure described in previous paragraph. When colloidal TiO_2 NPs were deposited on the CPP fabrics prior to loading of colloidal Ag NPs (CPP + TiO_2 + Ag), only the order of described procedures was switched.

The photocatalytic activity of TiO_2 NPs deposited on non-woven PP fabric pre-treated with corona discharge was examined in aqueous solution of acid dye C.I. Acid Orange 7 (AO7, Cassella). Chemical structure of AO7 is shown in Fig. 1. AO7 is monoazo dye with one sulfonate group.

HCl (Zorka, Serbia) and NaOH (Zorka, Serbia) were used to adjust pH of dye solution.

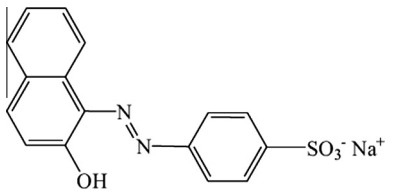

Fig. 1. Chemical structure of dye C.I. Acid Orange 7.

2.2. Methods

The morphology of the PP fibers was analyzed by scanning electron microscope JEOL JSM-6610LV. The samples were coated with a thin layer of Au prior to the analysis.

The total content of Ti in the CPP samples loaded with TiO_2 NPs was quantitatively determined using a Perkin Elmer 403 atomic absorption spectrometer (AAS).

Sonophotocatalytic degradation experiments were performed in accordance with a following procedure: 0.25 g of CPP + TiO_2, CPP + Ag + TiO_2, CPP + TiO_2 + Ag and CPP + TiO_2 × 2 samples were put into 50 mL of AO7 solution (10 mg/L). The beaker with a sample was placed in the ultrasonic bath operating at 40 kHz (Vims electric, Serbia) and it was illuminated by ULTRA-VITALUX lamp (300 W, Osram). The applied lamp provides sun-like irradiation. The distance between the lamp and the sample was set to 45 cm. Optical power was measured using R-752 Universal Radiometer Readout with sensor model PH-30, DIGIRAD and it was 30 mW cm^2. The concentration of AO7 solution after 30, 60, 90, 120, 150, 180, 210, 240 and 270 min of illumination was determined by measuring absorption intensity at λ_{max} = 484 nm using an UV–VIS spectrophotometer Cary 100 Scan (Varian). The percentage of dye removal was calculated according to following expression:

$$\text{Dye removal, } (\%) = \frac{(C_0 - C)}{C_0} \times 100 \quad (1)$$

where C_0 is the initial concentration of dye solution and C is the concentration of dye solution at investigated time.

The same procedure was also performed without illumination (sonocatalysis) and with illumination but without ultrasound (photocatalysis). After 3 h long photocatalysis the temperature of the dye solution increased from 21 to 27 °C. In order to avoid excessive heating of the system water in the ultrasonic bath was regularly changed during the sonocatalysis and sonophotocatalysis.

In order to get insight into absorption rate of the dye AO7 on the samples, described procedure was conducted in the dark, without illumination and ultrasound, but the beakers with dye solution were vigorously shaken.

In order to evaluate a possible reusability of modified CPP samples, described procedure was repeated two more times.

Total organic carbon (TOC) was determined in accordance with standard SRPS ISO 8245:2007 using a PPM LABTOC Analyser (software version 2.08). Organic carbon was oxidized to carbon dioxide through combustion in the presence of $Na_2S_2O_8$ in acidic medium (H_3PO_4) and under UV irradiation. Carbon-dioxide was directly measured by IR spectrometry.

3. Results and discussion

Surface morphology of PP fibers before and after corona treatment was characterized in SEM. SEM micrographs of PP and CPP fibers are shown in Fig. 2. It is evident that corona treatment causes significant morphological changes. Smooth surface is typical for untreated PP fibers (Fig. 2a). Surface of the PP fibers became rough after the corona treatment as a result of bombardment of different plasma species. Corona-induced droplet-like topography [26] is visible in Fig. 2b. Such droplet-like structure could not made by polymer melting during corona treatment [27,28] and it is likely to be a result of plasma oxidation and polymer chain scission on the fiber surface i.e., the formation of low-molecular-weight oxidized materials (LMWOMs) [28]. Agglomeration of those oligomers on the fiber surface could cause creation of the globules that give the specific droplet-like topography. In addition, SEM micrograph (inset to Fig. 2b) shows that some fiber segments are lifting from

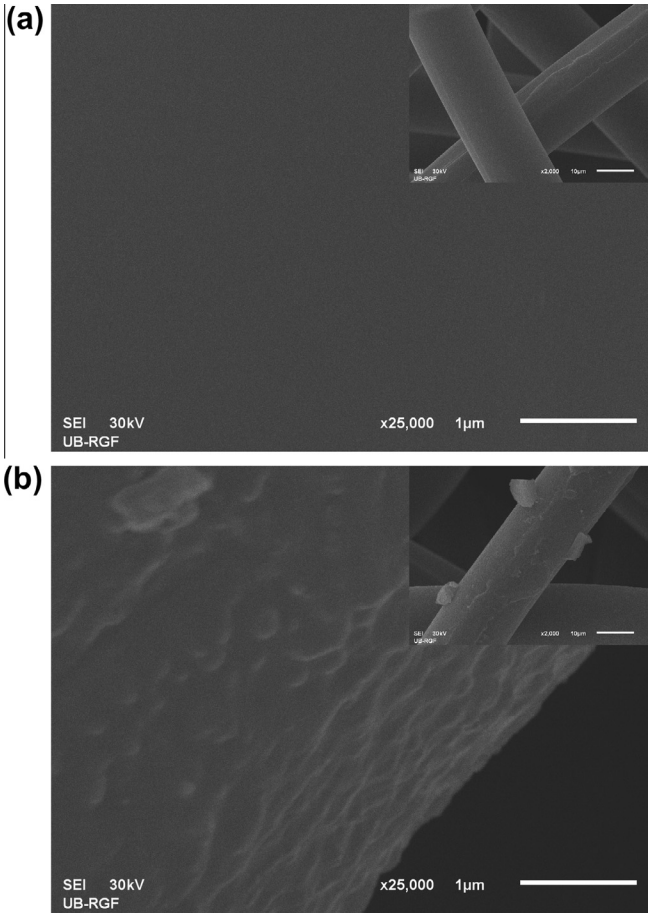

Fig. 2. SEM images of (a) PP and (b) CPP fibers.

the fiber surface. Similar morphological changes were noticed on the PP films and non-woven fabrics after dielectric barrier discharge (DBD) treatment at atmospheric pressure [21,28,29].

Corona treatment also induces the changes in chemical composition of the fiber surface layer by introducing polar functional groups (hydroxyl, carbonyl and carboxyl) [29,30]. The formation of polar functional groups on the PP fiber surface results in increased hydrophilicity. PP fibers are hydrophobic in nature and hence, the wetting time of untreated PP non-woven fabric was longer than 2 h. After corona treatment water droplet immediately wetted the CPP non-woven fabric surface. Consequently, hydrophilized PP fibers became more accessible to hydrophilic colloidal TiO_2 and Ag NPs. Another benefit of corona treatment corresponds to formation of hydroxyl and carboxyl groups that are expected to be the potential active sites for binding of TiO_2 NPs [26,31]. Our previous research also pointed out that activation of PP fibers by air RF plasma improved the binding efficiency of Ag NPs [32]. Fig. 3 shows SEM micrograph and EDX spectra of the CPP + Ag + TiO_2 fiber. Keeping in mind that the size of individual TiO_2 and Ag NPs in the colloidal solutions was approximately 6 and 10 nm [33,34], respectively, it is obvious that NPs agglomerated on the CPP fiber surface during impregnation. EDX spectra of randomly chosen NPs on the CPP + Ag + TiO_2 fiber surface revealed that both Ag and Ti are detected in each nanoparticle. This finding is crucial for further conclusions on the role of Ag NPs in the photocatalytic action of TiO_2 NPs.

The total amount of TiO_2 deposited on differently modified CPP non-woven fabrics was calculated on the basis of Ti content measured by AAS. These values are given in Table 1. Apparently, almost the equal amount of TiO_2 was found in the CPP + TiO_2 and

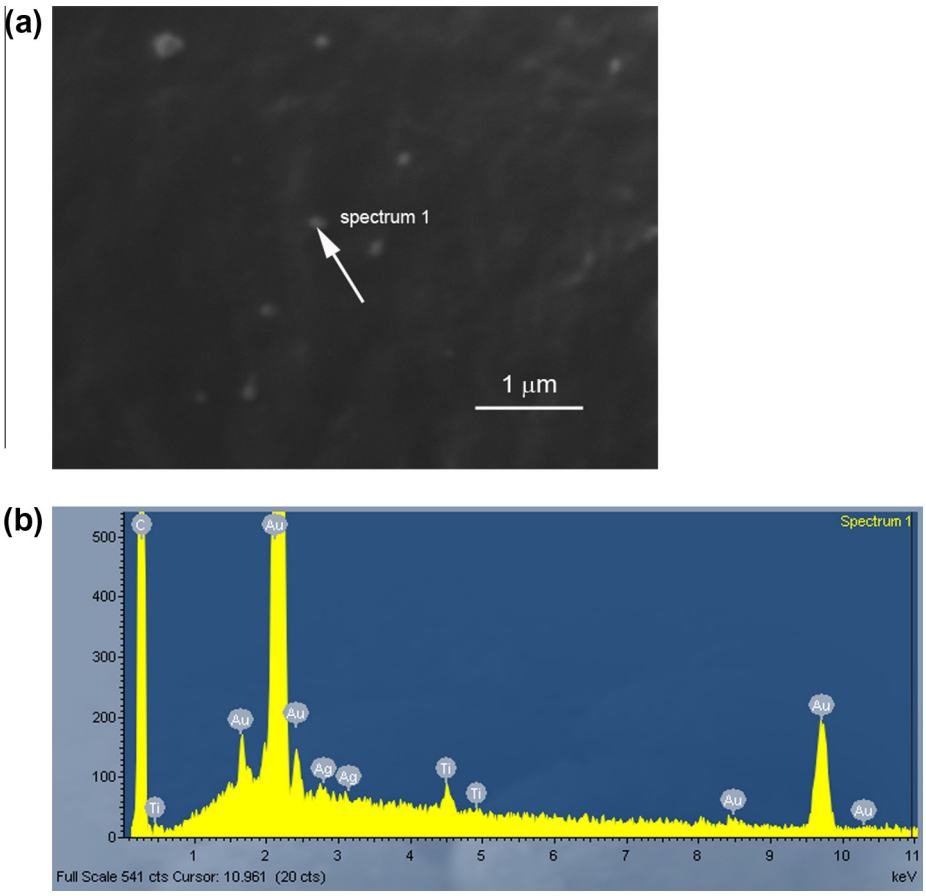

Fig. 3. SEM image of (a) the CPP + Ag + TiO_2 fiber and (b) EDX spectra of the deposited nanoparticle.

CPP + Ag + TiO_2 samples. Slightly smaller amount of TiO_2 was detected in the CPP + TiO_2 + Ag sample indicating that the order of NPs loading affects the deposition of TiO_2 NPs. The CPP + TiO_2 × 2 sample contains approximately by 63% more TiO_2 than the CPP + TiO_2 sample.

The sorption of dye AO7 from aqueous solution was studied in the dark. The equilibrium was reached already after 1 h of sorption. After 180 min of sorption 2.9% of dye was removed from the solution with the CPP + Ag + TiO_2 and CPP + TiO_2 + Ag samples. In case of the CPP + TiO_2 and CPP + TiO_2 × 2 samples, 4.0% and 21% of dye was removed from solution, respectively. Significantly higher dye uptake of the CPP + TiO_2 × 2 sample is due to larger amount of deposited TiO_2 NPs and more pronounced electrostatic interaction between the positively charged TiO_2 NPs and negatively charged dye anions. This will be discussed later in the text in more detail.

Before sonocatalysis, photocatalysis and sonophotocatalysis experiments, the stability of dye AO7, and possible photolysis and sonolysis were investigated. The aqueous solution of dye AO7 was exposed to ultrasound or lamp simulating the sun-like irradiation and the change of dye concentration was monitored using UV/VIS spectrophotometer. Nor photolysis neither sonolysis occurred.

Table 1
The total amount of TiO_2 in differently modified CPP samples.

Sample	TiO_2, mg/g
CPP + TiO_2	15.3
CPP + Ag + TiO_2	15.4
CPP + TiO_2 + Ag	13.9
CPP + TiO_2 × 2	25.0

Photocatalytic efficiency of TiO_2 NPs deposited on the CPP samples was also evaluated in aqueous solution of dye AO7. Dye removal efficiencies for the CPP + TiO_2, CPP + Ag + TiO_2, CPP + TiO_2 + Ag and CPP + TiO_2 × 2 samples after sonocatalysis, photocatalysis and sonophotocatalysis are shown in Fig. 4. The CPP + TiO_2 sample ensured complete removal of dye from both solution (Fig. 4a) and sample (Fig. 5) after 270 min long sonophotocatalysis. Fig. 4a also reveals that for the same duration of sonocatalysis and photocatalysis, the CPP + TiO_2 sample removed only about 37% and 62% of dye from the solution, respectively. Similar trend is observed after 240 min of sonophotocatalysis, sonocatalysis and photocatalysis in the presence of the CPP + Ag + TiO_2 sample (Figs. 4b and 5). Although the CPP + TiO_2 and the CPP + Ag + TiO_2 samples contain the same amount of TiO_2 (Table 1), the CPP + Ag + TiO_2 sample demonstrated higher sonophotocatalytic rate. This could be attributed to the presence of Ag NPs. Generally, it is suggested that doping of TiO_2 NPs with silver or depositing Ag NPs on TiO_2 NPs enhances the photocatalytic activity of TiO_2 NPs. Ag NPs act as electron scavengers inhibiting the recombination of photo-excited holes and electrons [35]. Fig. 5 shows that the CPP + TiO_2 and the CPP + Ag + TiO_2 samples were redder after photocatalysis and particularly after sonocatalysis due to adsorbed dye that did not degrade.

Fig. 4c reveals that in the presence of the CPP + TiO_2 + Ag sample about 73%, 24% and 45% of dye is removed from the solution after 270 min of sonophotocatalysis, sonocatalysis and photocatalysis, respectively. Despite incomplete discoloration of dye solution, the sonophotocatalytic efficiency of the CPP + TiO_2 + Ag sample was still satisfactory.

Lower sonophotocatalytic, sonocatalytic and photocatalytic rates in the presence of the CPP + TiO_2 + Ag sample compared to

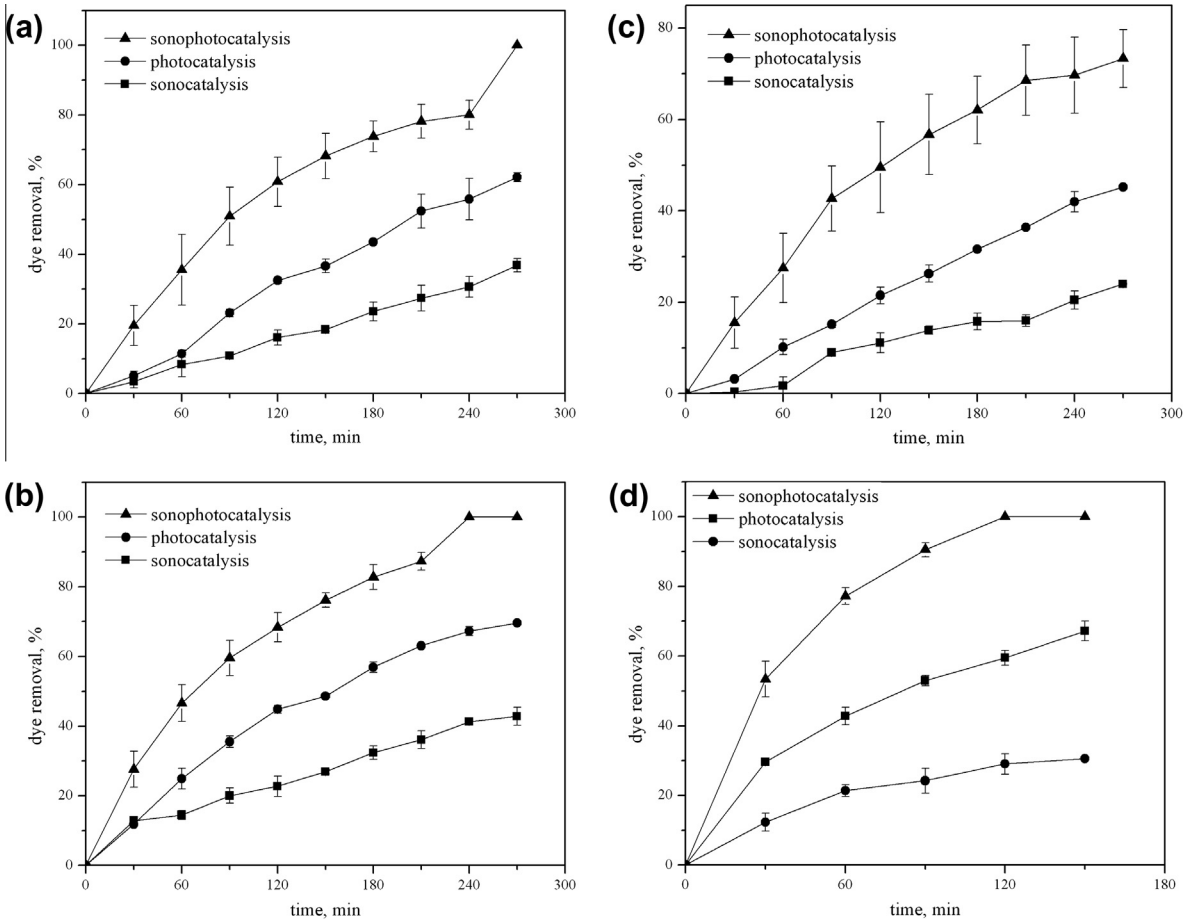

Fig. 4. Dye AO7 removal from the aqueous solution by different advanced oxidation processes in the presence of (a) CPP + TiO_2, (b) CPP + Ag + TiO_2, (c) CPP + TiO_2 + Ag and (d) CPP+TiO_2 × 2 samples.

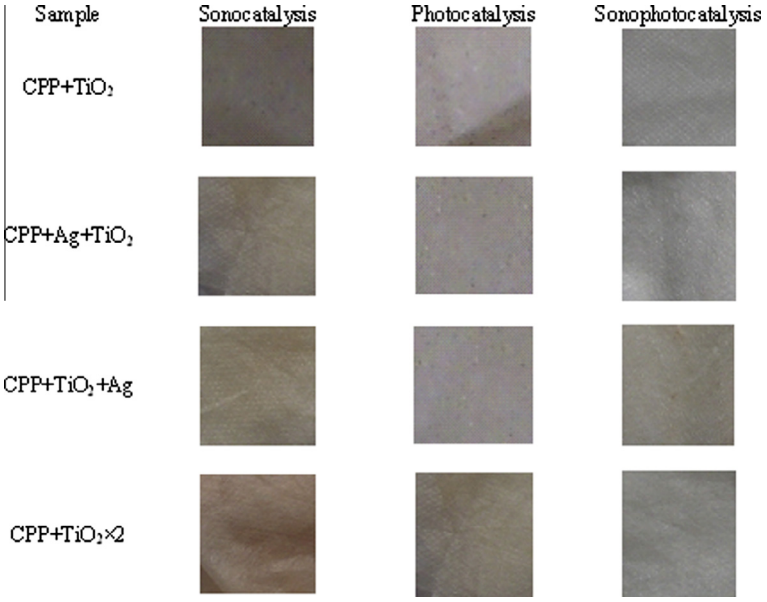

Fig. 5. Images of differently modified CPP after degradation of dye AO7 in aqueous solution.

the CPP + Ag + TiO_2 sample is very likely because Ag NPs on the CPP + TiO_2 + Ag sample are exposed to surrounding aqueous medium. Therefore, Ag NPs may hinder the action of TiO_2 NPs by inhibiting the potential reactions of generated holes and electrons with water molecules and O_2 which would otherwise result in formation of desired reactive species responsible for the dye degradation.

Complete discoloration of dye solution was achieved in the presence of the CPP + TiO_2 × 2 sample only after 150 min of sonophotocatalysis (Fig. 4d). White color of the CPP + TiO_2 × 2 sample (Fig. 5) implies that no dye residues remained in the system after sonophotocatalysis. Such result was expected because the CPP + TiO_2 × 2 sample contains about 60% more TiO_2 compared to the rest of the examined samples (Table 1). In contrast, for the same time of sonocatalysis and photocatalysis, about 70% and 40% of dye remained undegraded, respectively. This explains the red color of these samples (Fig. 5).

Apparently, sonophotocatalysis demonstrated superior dye degradation ability compared to sonocatalysis and photocatalysis, which is in accordance with literature data [4,3,8–10,24–32,35–39]. Sonophotocatalysis relies on two types of irradiation: UV and ultrasonic. When a surface of TiO_2 NPs is irradiated with light energy equal or larger than its bandgap energy ($E \geqslant 3.2$ eV), conduction band electrons (e^-_{cb}) and valence band holes (h^+_{vb}) are generated [9,13,35,40]. Photo-excited electrons and holes could either recombine or react with surrounding molecules. These electron–hole pairs react with molecules such as H_2O and O_2 producing very reactive radicals ($OH^{\cdot}$, $O_2^{\cdot-}$) that are responsible for dye degradation. In addition to these reactions, dye degradation could be also carried out directly by oxidation with holes or reduction with electrons.

At the same time, aqueous solution of dye undergoes ultrasonic irradiation through creation of acoustic cavitations [1,36,41]. Newly formed microbubbles grow and subsequently collapse leading to a generation of extremely high local temperatures and pressure rise [6]. Under these extreme conditions primarily hydroxyl ($OH^{\cdot}$) and hydrogen ($H^{\cdot}$) radicals followed by hydroperoxyl radicals ($HO_2^{\cdot}$) and hydrogen peroxide are generated. Higher concentration of reactive species, in particular $OH^{\cdot}$ radicals, is produced during sonophotocatalysis compared to sonocatalysis and photocatalysis alone [9,11,41]. It was reported that the AO7 degradation begins with attack of $OH^{\cdot}$ radicals when hydroxylated intermediaries are generated [42]. Thus, it was expected that degradation of dye is progressive during sonophotocatalysis [42].

As already mentioned, sonophotocatalysis is the combination of two processes: sonocatalysis and photocatalysis. In order to quantify the individual effects of sonocatalysis and photocatalys on the sonophotocatalysis, the synergy index (SynI) was calculated. The synergy index is expressed as a ratio between kinetic constant of the sonophotocatalysis and the sum of kinetic constants of the sonocatalysis and the photocatalysis (Eq. (2)) [10,36].

$$\mathrm{SynI} = \frac{k(\text{sonophotocatalysis})}{k(\text{sonocatalysis}) + k(\text{photocatalysis})} \quad (2)$$

If SynI is less than one, sonophotocatalysis is result of additive effect of sonocatalysis and photocatalysis. On the contrary, in case that the SynI is greater than one, synergistic degradation effect is predominant. According to literature data sonocatalysis, photocatalysis and sonophotocatalysis can be described by a pseudo-first order kinetic model [1,10,36,37]. Pseudo-first order rate constants and SinI values are presented in Table 2.

Obviously, for all investigated samples calculated value of SynI was greater than one indicating that during the sonophotocatalysis of dye AO7 synergistic degradation effect has been obtained. It is also noticeable that SinI for the CPP + TiO_2 + Ag sample was higher than for the CPP + TiO_2 and the CPP + Ag + TiO_2 samples even though the CPP + TiO_2 + Ag sample exhibited lower sonophotocatalytic efficiency. In comparison with the CPP + TiO_2 and the CPP + Ag + TiO_2 samples, the CPP + TiO_2 + Ag sample shows lower values of kinetic rates for the photocatalysis and sonocatalysis which significantly affected the calculated SynI value.

Sonophotocatalytic degradation of dye strongly depends on initial pH value of the solution [41]. Therefore, sonophotocatalytic degradation of dye AO7 in the presence of differently modified CPP non-woven materials was additionally evaluated in acidic (pH 4.0) and alkaline (pH 9.0) conditions. Fig. 6 demonstrates the influence of initial pH on sonophotocatalytical degradation efficiency of dye AO7 in aqueous solution.

It is evident that sonophotocatalytic degradation rate of dye AO7 was significantly promoted in acidic conditions. Complete discoloration of the solution was achieved already after 150 min with the CPP + TiO_2 sample in acidic conditions (Fig. 6a). This is approximately by 30% faster discoloration compared to the process performed in dye solution with initial pH 6.20. Complete discoloration of dye solution was also obtained in the case of CPP + Ag + TiO_2 sample but already after 120 min of sonophotocatalysis (Fig. 6b). Compared to low degradation efficiency in control (pH 6.20, Fig. 4c) and alkaline dye solutions (Fig. 6c) the CPP + TiO_2 + Ag sample ensured complete discoloration of dye solution in acidic medium after 150 min of sonophotocatalysis. The CPP + TiO_2 × 2 sample provided complete discoloration already after 90 min of sonophotocatalysis in acidic dye solution (Fig. 6d) whereas in alkaline conditions only about 30% of dye was degraded for the same period. Equivalent results are available in literature [38,41].

As an anionic dye AO7 is negatively charged due to presence of sulfonate group in its structure (Fig. 1) [38]. The point of zero charge of colloidal TiO_2 NPs is 5.2. Hence, the surface of TiO_2 NPs becomes positively charged below this pH value or negatively charged above it [38,41,43]. Consequently, acidic conditions would favor the electrostatic interaction between the positively charged TiO_2 NPs and negatively charged dye anions resulting in better dye adsorption and subsequent dye degradation. On the other hand, in alkaline conditions repulsion between negatively charged surface of TiO_2 NPs and dye anions becomes dominant leading to low degradation efficiency.

In order to investigate the possibility of reusing the CPP material modified with colloidal TiO_2 and Ag NPs, sonophotocatalytic processes were repeated two more times under the same conditions (pH 6.20). The kinetics of degradation of dye AO7 in aqueous solution during sonophotocatalysis is presented in Fig. 7. In comparison with the 1st cycle when the dye was completely removed from the solution, after the 2nd and the 3rd cycle, the dye removal

Table 2
The pseudo-first rate constants and synergy index of dye AO7 degradation in the presence of differently modified PP non-woven fabrics in aqueous solution.

Sample	Sonocatalysis		Photocatalysis		Sonophotocatalysis		SynI
	$k_1 \times 10^{-3}$ min^{-1}	R_1^2	$k_2 \times 10^{-3}$, min^{-1}	R_2^2	$k_3 \times 10^{-3}$, min^{-1}	R_3^2	
CPP + TiO_2	1.54	0.994	3.38	0.993	7.24	0.997	1.47
CPP + Ag + TiO_2	2.16	0.994	4.61	0.998	9.78	0.999	1.44
CPP + TiO_2 + Ag	0.95	0.984	2.16	0.996	5.24	0.995	1.69
CPP + TiO_2x2	3.13	0.976	7.13	0.993	25.01	0.999	2.44

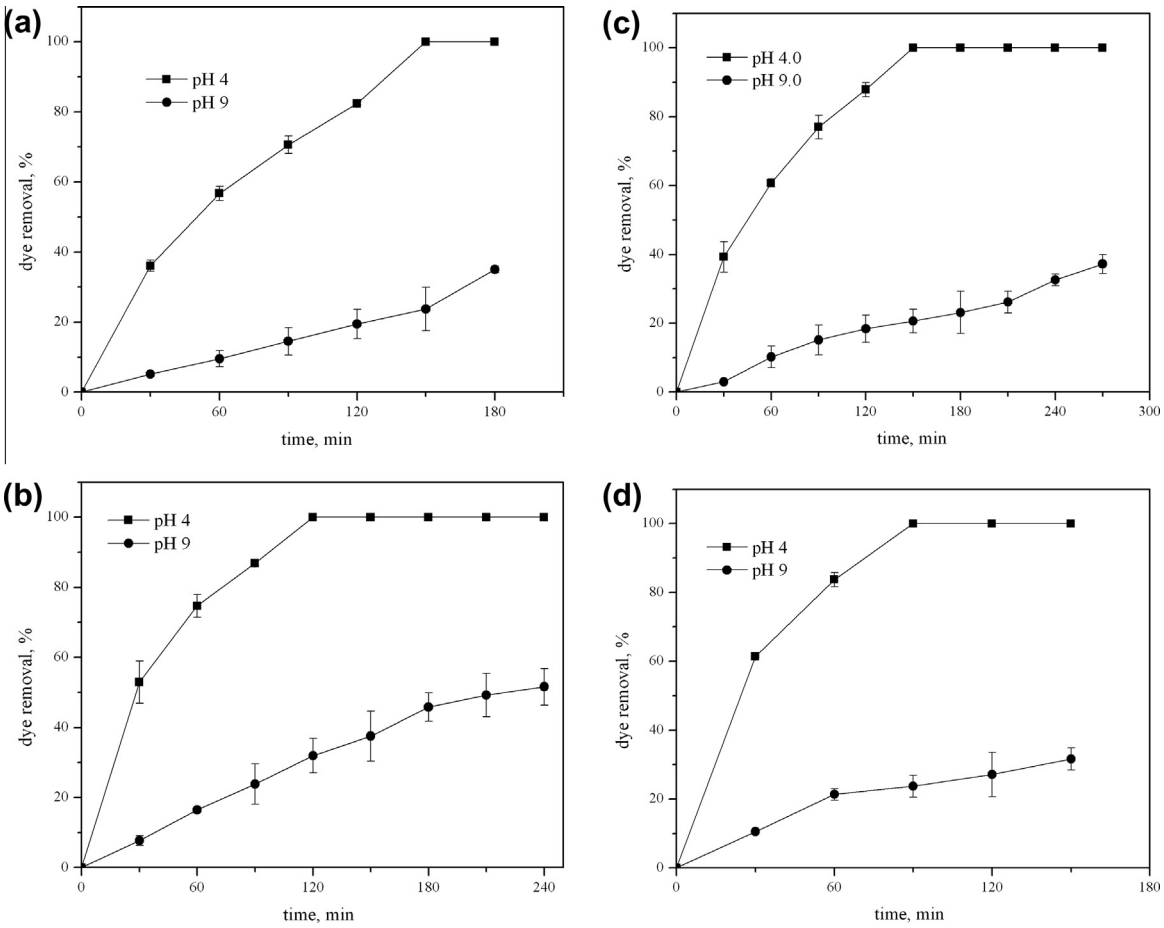

Fig. 6. Influence of pH value on the sonophotocatalytic degradation of dye AO7 in the presence of (a) CPP + TiO_2, (b) CPP + Ag + TiO_2, (c) CPP + TiO_2 + Ag and (d) CPP + TiO_2 × 2 samples.

efficiency in the presence of the CPP + TiO_2 sample decreased to 86% and 64%, respectively (Fig. 7a). Dye removal efficiency after the 2nd and the 3rd cycle in the presence of the CPP + Ag + TiO_2 sample decreased by 6% and 21%, respectively (Fig. 7b). Significant drop in degradation efficiency after the 2nd and the 3rd cycle occurred in the case of CPP + TiO_2 × 2 sample as shown in Fig. 7c. Observed general decrease in degradation efficiency was likely due to some desorption of TiO_2 NPs from the surface of non-woven fabrics during the repeated sonophotocatalytic cycles. This was particularly prominent in the case of CPP + TiO_2 × 2 sample possibly as a consequence of higher TiO_2 content on its surface (Table 1). Although the CPP + TiO_2 and the CPP + Ag + TiO_2 samples contain the same amount of TiO_2 (Table 1) the CPP + Ag + TiO_2 sample exhibited higher sonophotocatalytic activity in repeated cycles. This can be attributed to the presence of Ag NPs as they decrease the recombination rate of TiO_2 photo-excited charge carriers [35].

Presented results pointed out that corona pretreated PP non-woven material loaded with TiO_2 and TiO_2 and Ag NPs successfully removed dye AO7 from solution after 240–270 min of sonophotocatalysis. Apparently, the dye removal was achieved and the system became transparent but the question was posed whether the water was really purified. In order to evaluate the degree of water purification TOC values were measured. Several studies examined the TOC values during and after sonophotocatalytic degradation of different dye solutions [3,4,44,45]. General conclusion was established that TOC values decreased more slowly than discoloration rate [44]. Table 3 shows TOC values during and after sonophotocatalysis of dye AO7 in the presence of the CPP + TiO_2 and the CPP + Ag + TiO_2 samples. Initial TOC value of dye solution was 4.35 mg/L. Obviously, TOC values after sonophotocatalysis increased. Taking into account successful discoloration of dye solutions, these results were certainly unexpected. TOC value after sonophotocatalysis in the presence of the CPP + TiO_2 sample increased almost four times while in the presence of the CPP + Ag + TiO_2 sample, twice. Evidently, the variation of TOC value during the sonophotocatalytic degradation process in the presence of the CPP + Ag + TiO_2 sample was insignificant. In order to find out a possible explanation for such behavior, TOC values after sonophotocatalysis of distilled water in the presence of PP, CPP and CPP + TiO_2 samples were measured.

It was found that after being exposed to simultaneous UV and ultrasonic irradiation, PP material degraded and it contaminated the water (TOC = 4.90 mg/L). Generated reactive radicals may attack the polymer chain causing the formation of new radicals that further react with oxygen when mixture of different products is produced [46]. Corona treatment of PP brought about almost four times higher TOC values (TOC = 22.4 mg/L) compared to PP non-woven fabric. This could be due to loosely bound LMWOMs to polymer surface that were created during corona treatment. These oligomers can be removed by rinsing in the polar solvent [21]. It is very likely that their removal in water has been facilitated in the presence of UV and ultrasonic irradiation. However, the impregnation of CPP with TiO_2 NPs led to a double decrease in TOC values (TOC = 11.8 mg/L) compared to CPP sample. Recent study by Dastjerdi and Mojtahedi indicated that TiO_2/Ag NPs improved the stability of PP fabric against UV degradation [47].

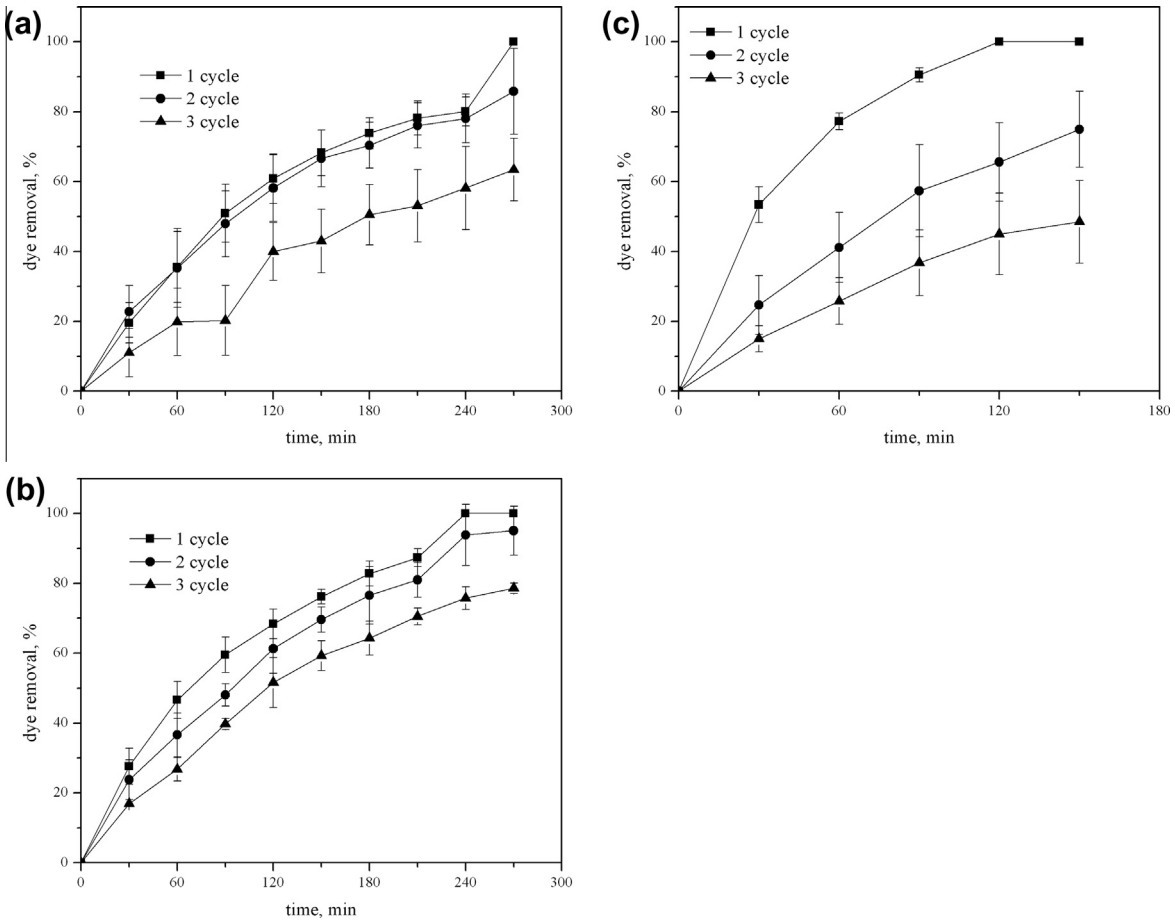

Fig. 7. Dye AO7 removal during repeated sonophotocatalytic processes in the presence of (a) CPP + TiO_2, (b) CPP + Ag + TiO_2 and (c) CPP + TiO_2 × 2 samples (pH 6.20).

Table 3
TOC values of dye AO7 solutions in the presence of the CPP + TiO_2 and the CPP + Ag + TiO_2 samples during and after sonophotocatalysis.

Sample	Time of sonophotocatalysis, min	TOC, mg/L
CPP + TiO_2	270	14.1
CPP + Ag + TiO_2	60	9.18
	120	11.8
	180	10.2
	240	8.58

In spite of significantly decreased TOC value of water after sonophotocatalysis with the CPP + TiO_2 sample compared to CPP sample, TOC value was still unacceptably high. Further, a comparison between TOC values of the CPP + TiO_2 sample in water (11.8 mg/L) and CPP + TiO_2 in dye solution (14.1 mg/L) after 270 min of sonophotocatalysis at the same conditions and TOC value of initial dye solution (4.35 mg/L) implies that approximately 50% of dye was mineralized.

This final evaluation of TOC opens up new perspectives on selection of supports for TiO_2 NPs. It is clear that support itself in addition to high efficiency for holding TiO_2 NPs must be stable against simultaneous UV and ultrasonic irradiation. If this last condition is not fulfilled it can pollute the water even more seriously than dye alone. Therefore, it is recommended that TOC or COD (chemical oxygen demand) evaluations should become obligatory part of each study on dye solution discoloration using TiO_2 NPs incorporated into the supports by sonophotocatalysis.

4. Conclusions

The results of this study showed that corona discharge at atmospheric pressure could be successfully utilized for activation of polypropylene fiber surface in order to provide improved binding efficiency of colloidal TiO_2 and Ag nanoparticles. Sonophotocatalysis of dye C.I. Acid Orange 7 solution ensured higher degradation efficiency compared to sonocatalysis and photocatalysis alone. Faster dye removal was obtained in acidic conditions.

Corona pre-treated polypropylene non-woven fabric double loaded with TiO_2 nanoparticles exhibited the best degradation efficiency, but the evident release of TiO_2 nanoparticles in repeated degradation cycles makes this system practically unacceptable. Corona pre-treated polypropylene non-woven fabric loaded with Ag nanoparticles prior to deposition of TiO_2 nanoparticles also provided excellent degradation efficiency. Although this sample contained the same amount of TiO_2 as the one that was only loaded with TiO_2 nanoparticles, its sonophotocatalytic activity was more prominent. Such behavior was attributed to the presence of Ag nanoparticles that facilitated the charge separation. Although this system is ensured fast discoloration of dye solution, TOC values of water measured after sonophotocatalysis were not satisfactory. High TOC values indicated that corona treatment of polypropylene as well as subsequent UV and ultrasonic irradiation have adverse effect on TOC. Therefore, it is suggested to include TOC evaluation in each case study where different supports for TiO_2 nanoparticles are used as these nanoparticles might guarantee the dye removal from solution but the stability of support could be problematic causing even more serious environmental impact.

Acknowledgement

The financial support for this work was provided by the Ministry of Education, Science and Technological Development of Republic of Serbia (Projects Nos. 45020 and 172056).

References

[1] Y.L. Pang, A.Z. Abdullah, S. Bhatia, Review on sonochemical methods in the presence of catalysts and chemical additives for treatment of organic pollutants in wastewater, Desalination 277 (2011) 1–14.
[2] M. Jagannathan, F. Grieser, M. Ashokkumar, Sonophotocatalytic degradation of paracetamol using TiO_2 and Fe^{3+}, Sep. Purif. Technol. 103 (2013) 114–118.
[3] J. Madhavan, P.S.S. Kumar, S. Anandan, F. Grieser, M. Ashokkumar, Degradation of acid red 88 by the combination of sonolysis and photocatalysis, Sep. Purif. Technol. 74 (2010) 336–341.
[4] Y. Wang, D. Zhao, W. Ma, C. Chen, J. Zhao, Enhanced sonocatalytic degradation of azo dyes by Au/TiO_2, Environ. Sci. Technol. 42 (16) (2008) 6173–6178.
[5] Y.G. Adewuyi, Sonochemistry in environmental remediation. 2. Heterogeneous sonophotocatalytic oxidation processes for the treatment of pollutants in water, Environ. Sci. Technol. 39 (2005) 8557–8570.
[6] C.G. Joseph, G.L. Puma, A. Bono, D. Krishnaiah, Sonophotocatalysis in advanced oxidation process: a short review, Ultrason. Sonochem. 16 (2009) 583–589.
[7] N.N. Mahamuni, Y.G. Adewuyi, Advanced oxidation processes (AOPs) involving ultrasound for waste water treatment: a review with emphasis on cost estimation, Ultrason. Sonochem. 17 (2005) 990–1003.
[8] H. Wang, J. Niu, X. Long, Y. He, Sonophotocatalytic degradation of methyl orange by nano-sized Ag/TiO_2 particles in aqueous solution, Ultrason. Sonochem. 15 (2008) 386–392.
[9] T. An, H. Gu, Y. Xioung, W. Chen, X. Zhu, G. Sheng, J. Fu, Decolourization and COD removal from reactive dye-containing wastewater using sonophotocatalytic technology, J. Chem. Technol. Biotechnol. 78 (2003) 1142–1148.
[10] Z. Cheng, X. Quan, Y. Xiong, L. Yang, Y. Huang, Synergistic degradation of methyl orange in an ultrasound intensified photocatalytic reactor, Ultrason. Sonochem. 18 (2012) 1027–1032.
[11] N.K. Boutoumi, H. Boutoumi, H. Khalaf, B. David, Synthesis and characterization of TiO_2- montmorillonite/polythiophene-SDS nanocomposites: application in the sonophotocatalytic degradation of rhodamine 6G, Appl. Clay Sci. 80–81 (2005) 56–62.
[12] M.A. Nawi, S.M. Zain, Enhancing the surface properties of immobilized Degusa-P25 TiO_2 for the efficient photocatalytic removal of methylene blue from aqueous solution, Appl. Surf. Sci. 258 (2012) 6148–6157.
[13] D. Markovic, B. Jokic, Z. Saponjic, B. Potkonjak, P. Jovancic, M. Radetic, Photocatalytic degradation of Dye C.I. direct blue 78 using TiO_2 nanoparticles immobilized on wool-based nonwoven material, Clean-Soil, Air, Water 41 (10) (2013) 1002–1009.
[14] L.C. Chuang, C.H. Luo, Characterization of supported TiO_2-based catalysts green-prepared and employed for photodegradation of malodorous DMDS, Mater. Res. Bull. 48 (2013) 238–244.
[15] H. Han, R. Bai, Highly effective buoyant photocatalyst prepared with a novel layered-TiO_2 configuration on polypropylene fabric and the degradation performance for methyl orange dye under UV–VIS and Vis light, Sep. Purif. Technol. 73 (2010) 142–150.
[16] J. Yang, J. Dai, C. Chen, J. Zhao, Effects of hydroxyl radicals and oxygen species on the 4-chlorophenol degradation by photoelectrocatalytic reactions with TiO_2-film electrodes, J. Photochem. Photobiol. A 208 (1) (2009) 66–77.
[17] A.H. El-Sheikh, Y.S. Al-Degs, A.P. Newman, D.E. Lynch, Oxidized activated carbon as support for titanium dioxide in UV-assisted degradation of 3-chlorophenol, Sep. Purif. Technol. 54 (1) (2007) 117–123.
[18] Y.X. Chen, K. Wang, L.P. Lou, Photodegradation of dye pollutants on silica gel supported TiO_2 particles under visible light irradiation, J. Photochem. Photobiol. A 163 (1–2) (2004) 281–287.
[19] J. Yun, J.S. Im, A. Oh, D.H. Jin, T.S. Bae, Y.S. Lee, H.I. Kim, PH-sensitive photocatalytic activities of TiO_2/poly(vinyl alcohol)/poly(acrylic acid) composite hydrogels, Mater. Sci. Eng. B Adv. 176 (3) (2011) 276–281.
[20] N. Yaman, E. Özdoğan, N. Seventekin, Effect of surrounded air atmospheric plasma treatment on polypropylene dyeability using cationic dyestuff, Fibers Polym. 14 (9) (2013) 1472–1477.
[21] K.G. Kostov, T.M.C. Nishime, L.R.O. Hein, A. Toth, Study of polypropylene surface modification by air dielectric barrier discharge operated at two different frequencies, Surf. Coat. Technol. 234 (2013) 60–66.
[22] S. Shahidi, B. Moazzenchi, M. Ghoranneviss, S. Azizi, Investigation on dyeability of polypropylene fabrics grafted with chitosan after plasma modification, Eur. Phys. J. Appl. Phys. 62 (2013) 10801.
[23] T. Rajh, A. Ostafin, O.I. Micic, D.M. Tiede, M.C. Thurnauer, Surface modification of small particles TiO_2 colloids with cysteine for enhanced photochemical reduction: an EPR Study, J. Phys. Chem. 100 (1996) 4538–4545.
[24] R.C. Thompson, Oxidation of peroxotitanium (IV) by chlorine and cerium (IV) in acidic perchlorate solution, Inorg. Chem. 23 (1984) 1794–1798.
[25] Z.V. Saponjic, R. Csencsits, T. Rajh, N. Dimitrijevic, Self-assembly of topo-derivatized silver nanoparticles into multilayer film, Chem. Mater. 15 (2003) 4521–4526.
[26] D. Mihailovic, Z. Saponjic, M. Radoicic, S. Lazovic, C.J. Baily, P. Jovancic, J. Nedeljkovic, M. Radetic, Functionalization of cotton fabric with corona/air RF plasma and colloidal TiO_2 nanoparticles, Cellulose 18 (2011) 811–825.
[27] M. Strobel, C.J. Lyons, The role of low-molecular-weight oxidized materials in the adhesion properties of corona-treated polypropylene film, J. Adhes. Sci. Technol. 17 (2003) 15–23.
[28] N. Radić, B.M. Obradović, M. Kostić, B. Dojčinović, M.M. Kuraica, M. Černák, Deposition of silver ions onto DBD and DCSB plasma treated nonwoven polypropylene, Surf. Coat. Technol. 206 (2012) 5006–5011.
[29] F. Leroux, C. Campagne, A. Perwuelz, L. Gengembre, Polypropylene film chemical and physical modifications by dielectric barrier discharge plasma treatment at atmospheric pressure, J. Colloid Interface Sci. 328 (2008) 412–420.
[30] R. Morent, N. De Geyter, C. Leys, L. Gengembre, E. Payen, Comparison between XPS- and FTIR-analysis of plasma-treated polypropylene film surfaces, Surf. Interface Anal. 40 (2008) 597–600.
[31] A. Bozzi, T. Yuranova, J. Kiwi, Self-cleaning of wool-polyamide and polyester textiles by TiO_2-rutile modification under daylight irradiation at ambient temperature, J. Photochem. Photobiol. A 172 (2005) 27–34.
[32] Z.Lj. Petrović, P. Maguire, M. Radmilović-Rađenović, M. Radetić, N. Puač, D. Marić, C. Mahony, G. Malović, On application of plasmas in nanotechnologies, in: A. Korkin, P.S. Krstić, J.C. Wells (Eds.), Nanotechnology for Electronics, Photonics, and Renewable Energy, Springer New York, USA, 2010, pp. 81–135 (ISBN 978-1-4419-7234-7).
[33] M. Radetić, V. Ilić, V. Vodnik, S. Dimitrijević, P. Jovančić, Z. Šaponjić, J.M. Nedeljković, Antibacterial effect of silver nanoparticles deposited on corona treated polyester and polyamide fabrics, Polym. Adv. Technol. 19 (2008) 1816–1821.
[34] D. Mihailović, Z. Šaponjić, M. Radoičić, T. Radetić, P. Jovančić, J. Nedeljković, M. Radetić, Functionalization of polyester fabrics with alginates and TiO_2 nanoparticles, Carbohydr. Polym. 79 (2010) 526–532.
[35] M. Radetic, Functionalization of textile materials with TiO_2 nanoparticles, J. Photochem. Photobiol. C 16 (2013) 62–76.
[36] N. Talebian, M.R. Nilforoushan, F.J. Mogaddas, Comparative study on the sonophotocatalytic degradation of hazardous waste, Ceram. Int. 39 (2013) 4913–4921.
[37] S.F. Xiong, Z.L. Yin, Z.F. Yuan, W.B. Yan, W.Y. Yang, Dual-frequency (20/40 kHz) ultrasonic assisted photocatalysis for degradation of methylene blue effluent: synergistic effect and kinetic study, Ultrason. Sonochem. 19 (2012) 756–761.
[38] N.J.B. Pérez, M.F.S. Herrera, Sonophotocatalytic degradation of congo red and methyl orange in the presence of TiO_2 as a catalyst, Ultrason. Sonochem. 14 (2007) 589–595.
[39] E. Selli, Synergistic effects of sonolysis combined with photocatalysis in the degradation of an azo dye, Phys. Chem. Chem. Phys. 4 (2002) 6123–6128.
[40] I.K. Konstantinou, T.A. Albanis, TiO_2-assisted photocatalytic degradation of azo dyes in aqueous solution kinetic and mechanistic investigations: a review, Appl. Catal. B 49 (2004) 1–14.
[41] Z. Eren, Ultrasound as a basic auxiliary process for dye remediation: a review, J. Environ. Manage. 104 (2012) 127–141.
[42] P. Bansal, D. Singh, D. Sud, Photocatalytic degradation of azo dye in aqueous TiO_2 suspension: reaction pathway and identification of intermediates products by LC/MS, Sep. Purif. Technol. 72 (2010) 357–365.
[43] T. Velegraki, I. Poulios, M. Charalabaki, N. Kalogerakis, P. Samaras, D. Mantzavinos, Photocatalytic and sonolytic oxidation of acid orange 7 in aqueous solution, Appl. Catal. B 62 (2006) 159–168.
[44] J. Madhavan, F. Grieser, M. Ashokkumar, Degradation of orange-G by advanced oxidation processes, Ultrason. Sonochem. 17 (2010) 338–343.
[45] Z. Eren, Degradation of an azo dye with homogeneous and heterogeneous catalysts by sonophotolysis, Clean-Soil, Air, Water 40 (11) (2012) 1284–1289.
[46] Z. Karami, M. Youssefi, S. Borhani, The effects of UV irradiation exposure on the structure and properties of polypropylene/ZnO nanocomposite fibers, Fibers Polym. 14 (2013) 1627–1634.
[47] R. Dastjerdi, M.R.M. Mojtahedi, Multifunctional melt-mixed Ag/TiO_2 nanocomposite PP fabrics: water vapour permeability, UV resistance, UV protection and wear properties, Fibers Polym. 14 (2013) 298–303.